Available online at www.sciencedirect.com
SCIENCE DIRECT®
C. R. Mecanique 334 (2006) 1–7
COMPTES RENDUS MECANIQUE
http://france.elsevier.com/direct/CRAS2B/

Attrition and particle breakage under monotonic and cyclic loading

Frédéric Mayoraz [a], Laurent Vulliet [b], Lyesse Laloui [b,*]

[a] *De Cérenville Géotechnique SA, 1024 Ecublens, Switzerland*
[b] *Soil Mechanics Laboratory, École Polytechnique Federale Lausanne, EPFL, Station 18, 1015 Lausanne, Switzerland*

Received 5 April 2005; accepted after revision 8 November 2005

Available online 13 December 2005

Presented by Évariste Sanchez-Palencia

Abstract

The morphological evolution of gravel grains under monotonic and cyclic loading, typically present in road structures, is presented. Two types of mineralogy are considered: a limestone and a sandstone. Loading in uniaxial strain conditions are applied, with a maximum mean pressure of 5 MPa and a maximum number of cycles of 250 000. Variations in grain size distribution and grain shape, measured with image analysis techniques, are discussed in detail. In the case of uniform grain size distribution, particle breakage does appear for stresses around 500 kPa for the limestone grains and 100 kPa for the sandstone grains. For well-graded materials under low cyclic pressures (<1 MPa), changes in grain size distribution can hardly be detected. ***To cite this article: F. Mayoraz et al., C. R. Mecanique 334 (2006).***

Résumé

Attrition et rupture de particules sous chargements monotones et cycliques. L'évolution de la morphologie de grains de sable soumis à des chargements monotones et cycliques, du type de celles sollicitant les structures routières est présentée. Deux minéralogies sont considérées : un calcaire et un grès. Les sollicitations sont appliquées en déformations uniaxiales, avec une pression moyenne maximale de 5 MPa et un nombre de cycle maximal de 250 000. Les variations de granulométrie et de forme de grains, mesurées à l'aide de techniques d'imagerie numériques sont discutées en détail. Dans le cas d'une granulométrie droite, les ruptures de grains apparaissent à des contraintes de l'ordre de 500 kPa pour le calcaire, de 100 kPa pour le grès. Dans le cas d'une granulométrie étendue, peu de changement sont détectés sous des faibles charges cycliques (<1 MPa). ***Pour citer cet article : F. Mayoraz et al., C. R. Mecanique 334 (2006).***

Keywords: Granular media; Cyclic loading; Morphology of gravels; Image analysis techniques; Grain size distribution

Mots-clés : Milieux granulaires ; Sollicitations cycliques ; Morphologie des sables ; Imagerie numérique ; Granulométrie

* Corresponding author.
E-mail address: lyesse.laloui@epfl.ch (L. Laloui).

1631-0721/$ – see front matter
doi:10.1016/j.crme.2005.11.001

1. Introduction

Road foundations are subjected to very complex loading conditions involving (hydro)mechanical, chemical and thermal cyclic effects. This strongly affects the behaviour at both short (resilient) and long (permanent) term, and is rather difficult to model. Empirical and, more recently, mechanical models have been used for road design (e.g., [1–3]) and a recent European COST effort has also focused on the behaviour of unbound granular materials [4]. As part of this program, the use of recycled material for unbound road foundations was considered and the delicate problem of particle breakage and attrition was raised among other questions. This paper addresses some of these points. Further considerations concerning characterisation, as well as modelling, of the behaviour of these materials are found in Mayoraz [5].

According to a study by Descoeudres et al. [6], in Switzerland, over the next 10 years, about 15% of the granular materials used in the construction industry will be recycled from excavation sites (mostly tunnelling). Based on historical data, 20% of these materials are expected to be used in road bases.

As a consequence, there is a need for improved characterisation of such materials whose mineralogy, grain shape and size do not necessarily meet the established standards [7].

This Note presents the tools and methods used to characterise the morphology of unbound granular materials and to analyse and experimentally observe grain breakage and attrition. Monotonic and cyclic tests in a large oedometer are presented.

2. Materials

Two materials and two grain size distributions were used in this study. The first material is a calcareous (limestone) gravel extracted by a tunnelling machine (TBM) during the excavation of the Varen Tunnel (Valais, Switzerland); its grain size distribution does not fit the standards for road construction. The second one is a sandstone-based gravel extracted from the quarry of Villarlod (Fribourg, Switzerland). Fig. 1 presents the various grain size distribution curves:

(i) raw Varen gravel;
(ii) curve G1 representing a reconstituted well-graded gravel fitting the requirements;
(iii) a reconstituted, poorly-graded gravel with grain diameter between 8 and 16 mm;
(iv) Swiss VSS standard band.

The simple compression strength R_c of both core materials is given in Table 1. It can be seen that the strength of the limestone is about three time that of the sandstone. This will later play an important role for particle breakage.

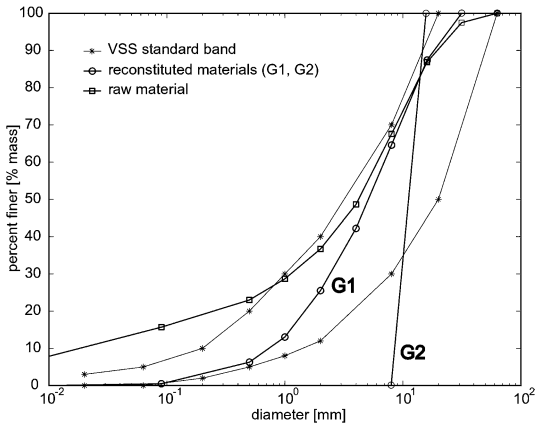

Fig. 1. Grain size distributions.
Fig. 1. Granulométrie des matériaux.

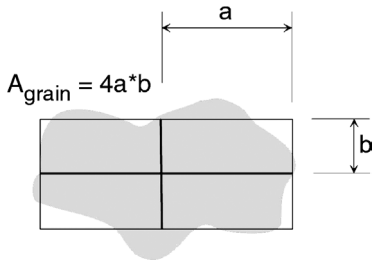

Fig. 2. Dimensions used to define sphericity.
Fig. 2. Grandeurs utilisées pour définir la sphéricité.

Table 1
Grains characteristics

	Roundness [–]	Sphericity [–]	Rc [Mpa]
Limestone	0.52	0.46	50–150
Sandstone	0.49	0.45	17–50

3. Morphology

Two morphological parameters are used here to describe the shape of gravel grains: sphericity and roundness.

Sphericity is defined as the ratio between the largest dimension of the grain (its length) and the mean of the dimensions normal to the length (see Fig. 2):

$$\text{Sphericity} = \frac{b}{2a} \tag{1}$$

Roundness is defined according to Krumbein using the Hough transform [8] as:

$$\text{Roundness} = \frac{\sum_{i=1}^{N} r_i}{R \cdot N} \tag{2}$$

where r_i are the radii detected by the Hough transform, N the number of detected circles and R the radius of the largest inscribed circle.

Roundness and sphericity values for the two gravels are given in Table 1. They are determined by using image processing techniques. Due to resolution, the sample is first divided into sub-fractions, about 50 grains at a time being placed on a translucent plate, avoiding contact between grains. Pictures are then taken using a digital camera.

Sphericity determination is rapid and easy using the IMAQVision libraries of LabVIEW®.

Roundness is determined using ad hoc software based on the Hough transform to detect the circles [8]. Using the digital image of a single grain, the distance r from any point (a_i, b_j) of the grain to its boundary can be calculated and is assumed to represent the radius of a circle (Fig. 3(a)). Further, a cumulative parameter $A(a_i, b_j, r)$ is computed. For each point, a 'winning' radius is found using a threshold function $T(r)$ (Fig. 3(b)). This function is introduced in order not to penalize the contribution of circles with small radii to the cumulative parameter. Finally, a local maximum search is undertaken using a mobile window (Fig. 3(c)). The end result of this procedure is presented in Fig. 3(d) and the value of the roundness coefficient is then determined using Eq. (2).

4. Preliminary tests and testing setup

4.1. Brewer's chart

In order to validate the implemented algorithm, a comparison test was performed with the results presented by Luo in 1995 and based on Brewer's chart (Fig. 4(a) and [9]).

Fig. 4(b) shows that the authors' absolute values differ slightly from those obtained by Luo but present the same trend. The capacity of the method to detect roundness variation is therefore demonstrated (here with a 2D example).

4.2. Severe sieving

As a preliminary test to assess grain shape changes due to mechanical effect, a sandstone-based gravel of grain size distribution G2 (Fig. 1) was subjected to severe sieving with violent shaking effects.

Morphological parameters were determined for about 40 grains. Fig. 5 clearly shows that the grains evolve towards more spherical shapes due to the severe mechanical treatment. Sphericity changed from 0.46 before to 0.58 after treatment and roundness changed from 0.52 to 0.62.

4.3. Oedometer device and sample preparation

Mechanical tests were performed using a large diameter oedometer (diameter 250 mm, see Fig. 6). In order to determine all the components of the stress tensor, strain gages were installed on the circumference of the cylinder.

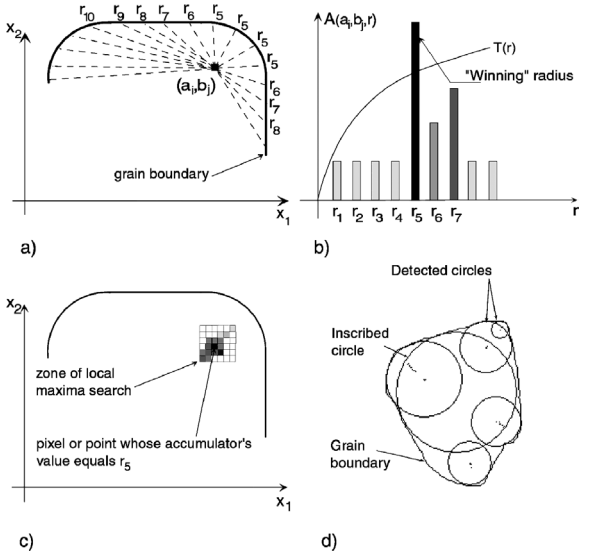

Fig. 3. (a) Calculating distances from point (a_i, b_j) to grain boundary; (b) cumulative parameter A at point (a_i, b_j) and threshold function $T(r)$; (c) local maxima search; (d) result of a Hough transform on a grain.

Fig. 3. (a) Calcul des distances de la bordure au point (a_i, b_j) ; (b) représentation de l'accumulateur A au point (a_i, b_j) et de la fonction de seuil $T(r)$; (c) recherche des maxima locaux ; (d) résultats d'une transformée de Hough sur un grain.

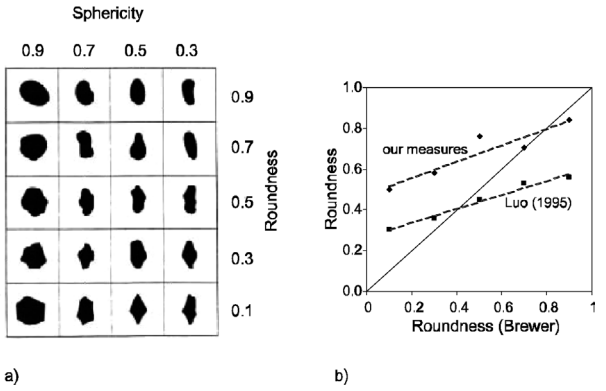

Fig. 4. (a) Brewer's chart; (b) roundness measurement of the grains of Brewer's chart based on the Hough transform: comparison of our measures and those done by Luo [8].

Fig. 4. (a) Abaque de Brewer ; (b) mesure de l'angularité des grains de l'abaque de Brewer à l'aide de la transformée de Hough : comparaison entre nos mesures et celles réalisées par Luo [8].

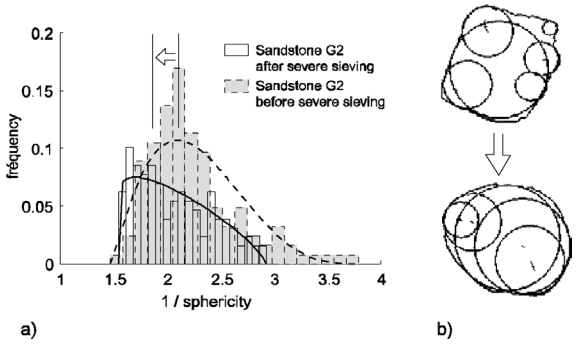

Fig. 5. Morphological parameters of Villarlod gravel before and after severe sieving: (a) sphericity: before = 0.46, after = 0.58; (b) roundness: before = 0.52, after = 0.62.

Fig. 5. Paramètres morphologiques du grès de Villarlod avant et après tamisage : (a) sphéricité : avant = 0,46, après = 0,58 ; (b) angularité : avant = 0,52, après = 0,62.

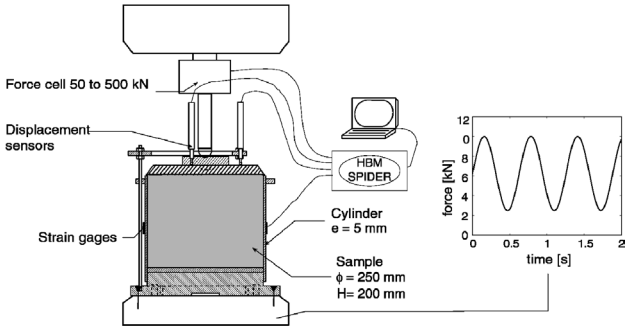

Fig. 6. Large oedometer setup and loading history.

Fig. 6. Schéma de l'oedomètre de grand diamètre et l'histoire de chargement.

Load-controlled conditions were applied. For the cyclic tests, a sinusoidal loading history was used, with a low frequency of 1 Hz.

Different sample preparation techniques were used. For the well-graded gravel (with G1 grain size distribution, see Fig. 1), compaction was obtained by dynamic loading using the standard Proctor procedure and energy. The initial water content was $w = 0.5\%$, the initial void ratio $e_0 = 0.40$ and the dry mass density $\rho_d = 1.9\ \mathrm{t/m^3}$.

Samples of uniform grain size distribution G2 were simply prepared by deposition in the mould.

5. Experimental results

The experimental program is summarised in Table 2. Monotonic and dynamic loading tests on the two materials with different grain size distributions are presented.

5.1. Monotonic and cyclic loading tests on Varen gravel

Fig. 7 shows grain size distribution curves determined before and after cyclic loading for the limestone-based calcareous Varen gravel and for the G1 and G2 grain size distribution (see Table 2). No significant attrition or particle breakage can be observed in the case of the well-graded grain size distribution G1. However, this phenomenon can be observed on the poorly graded grain size distribution G2, even after few cycles.

As a comparison, a monotonic loading test was performed on the same material type and grain size distribution G1. It was found that particle breakage started at a mean stress value of 5 MPa, a value never reached during the cyclic tests on G1. In Fig. 8, effects of particle breakage can be seen, but no signs of attrition can be detected (no production of fines).

A maximal mean pressure of 0.5 MPa during the cyclic tests on G1 represents about 10% of the value leading to grain breakage. Thus, this might ensure that no fatigue related effects will affect the behaviour of such a material. In the latter case, the maximal cyclic mean pressure is certainly greater than the value leading to grain breakage.

Fig. 9 shows the result of the cyclic loading. Hardly any changes in sphericity or roundness may be observed.

Table 2
Experimental program using the large oedometer

Materials	Grain-size distribution	p_{max}	
		Monotonic	Cyclic
Limestone	G1	5 MPa	0.12–0.25–0.5 MPa $N = 250\,000$
	G2	0.5–1–3 MPa	0.5 MPa $N = 100$
Sandstone	G1	–	–
	G2	0.5–1–3 MPa	–

The maximal value of the mean pressure is indicated.

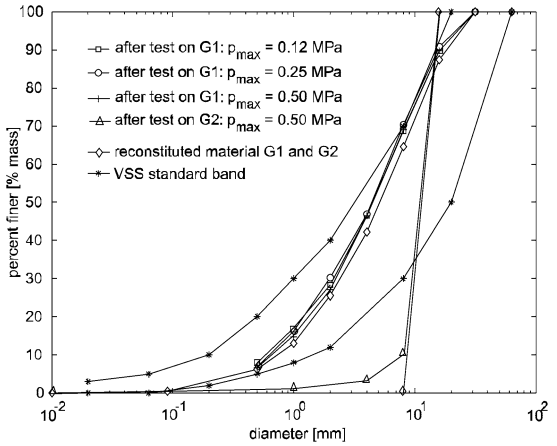

Fig. 7. Grain size distribution of Varen gravel after cyclic loading.

Fig. 7. Evolution granulométrique du sable de Varen après un chargement cyclique.

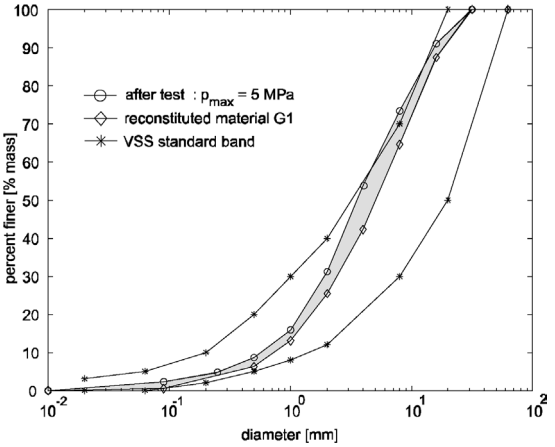

Fig. 8. Grain size distribution of Varen gravel after monotonic loading.

Fig. 8. Evolution granulométrique du sable de Varen après un chargement monotone.

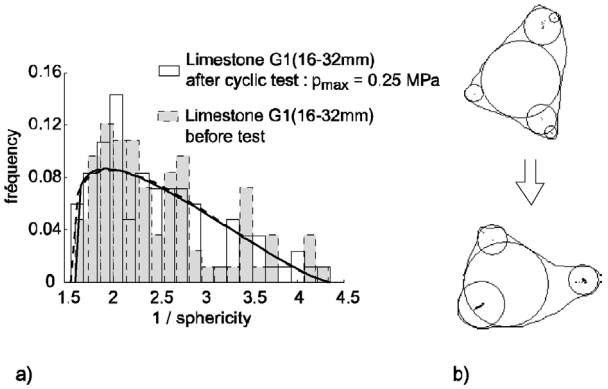

Fig. 9. Morphological parameters of the Varen gravel G2 before and after cyclic loading (a) sphericity (before = 0.45, after = 0.45); (b) roundness before = 0.49, after = 0.51).

Fig. 9. Paramètres morphologiques du sable de Varen G2 avant et après chargement cyclique : (a) sphéricité : avant = 0,45, après = 0,45 ; (b) angularité : avant = 0,49, après = 0,51.

5.2. Monotonic loading on poorly-graded (G2) samples

In order to observe the role of mineralogy on particle breakage, both materials were tested using poorly-graded samples. Indeed, micromechanical approaches show that grain size distribution has a significant influence on the amount of grain breakages [10]. In the case of similar macroscopic mechanical solicitations a poor grain size distribution is the most critical situation since the contact points between particles are a minimum in this case and the contact forces are then a maximum.

Fig. 10 shows the evolution of the grain size distribution for different values of the maximum reached mean pressure. It can be clearly seen that particle breakage increases with pressure and is more frequent for the weaker material (sandstone). In this latter case, crushing always produce sand grains whose size lies between 0.1 and 0.6 mm, corresponding to the size of those composing the sandstone.

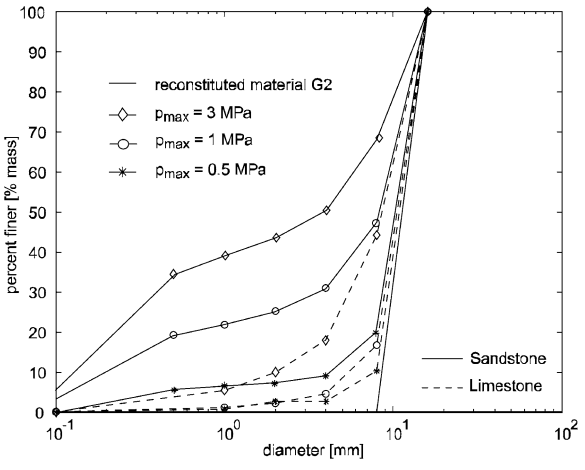

Fig. 10. Evolution of grain size distribution after monotonic loading at different large mean pressure and for the two material types and G2 grain size distribution.

Fig. 10. Evolution de la granulométrie après chargement monotone à fortes contraintes moyennes pour deux types de matériaux et granulométrie G2.

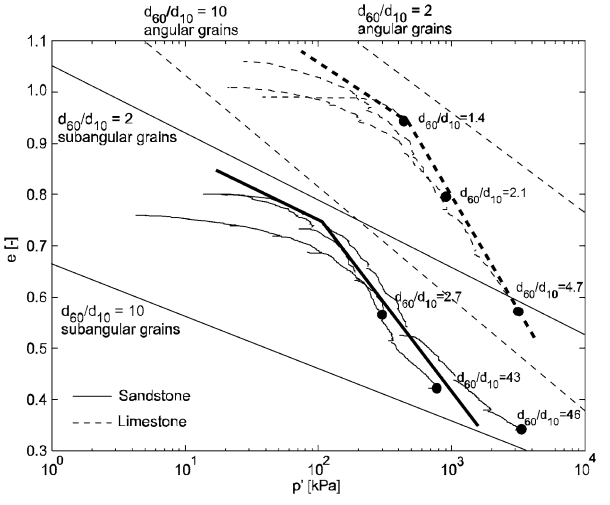

Fig. 11. Oedometer tests with grain breakage for both material types and G2 grain size distribution. Evolution of the compressibility index and comparisons with compressibility curves given by correlation (Biarez and Hicher [11]).

Fig. 11. Essais oedométriques avec rupture de grains pour les deux types de matériaux et granulométrie G2. Evolution de l'indice de compressibilité et comparaison avec les courbes de compressibilités données par corrélation (Biarez et Hicher [11]).

Biarez and Hicher [10] found that the position of the compression curve depends on the grading of the material as characterised by the coefficient of uniformity (d_{60}/d_{10}) as well as the angularity of the particles and proposed a correlation between these parameters. They also showed that the compressibility index rises when particle breakage appears, since material changes intrinsically.

In this study, the calcareous gravel is characterised as 'angular' and the sandstone as 'subangular'. The G2 grain size distribution curve has a ratio d_{60}/d_{10} of about 2.

Fig. 11 presents the superposition of the compressibility curves found by correlation and the results of the authors' tests. At first, it is shown that the initial void ratio is lower for subangular grains than for angular, which is coherent. Then, the compressibility index rises as soon as grain breakage occurs and crosses the loci of identical uniformity coefficients. It may be concluded that particle breakage does appear for stresses around 500 kPa for the limestone grains and 100 kPa for the sandstone grains. This shows that the maximal mean pressure reached during the cyclic test on the grain size distribution G2 of limestone gravel is greater than the value leading to grain breakage. Finally, the evolution of the uniformity coefficient is more coherent with the correlation for the limestone than that for the sandstone. In this latter case, the uniformity coefficient does not increase after 1 MPa despite the fact that breakage still occurs. This is due to the mineralogy of the sandstone (weakly-cemented sand grains), for which breakage is related to debonding of sand grains.

6. Conclusions

This paper presents the tools and methods used to characterise the morphology of unbound granular materials and to analyse and experimentally observe gain breakage and attrition.

Two morphological parameters are determined using image processing techniques to describe the shape of gravel grains: sphericity and roundness. Roundness is determined using an ad-hoc software based on the Hough transform.

A sandstone-based poorly-graded gravel subjected to severe sieving clearly shows that the grains evolve towards more spherical shapes. The limestone-based well-graded calcareous Varen gravel presents no significant attrition or particle breakage after 250 000 cycles of uniaxial loading.

Particle breakage under monotonic loading does appear for stresses above 500 kPa for the limestone grains and 100 kPa for the sandstone grains and the evolution of the compressibility index is coherent with other observed relations.

From a mechanical point of view, granular materials whose morphological characteristics do not meet the established standard could be used in road foundations construction, provided that grain size distribution is well-graded.

Acknowledgements

The Authors thank the Swiss Office for Science and Education for its support in the context of the COST 337 action.

References

[1] J.-L. Paute, P. Hornych, J.-B. Benaben, Comportement mécanique des graves non traitées, Bulletin de liaison des Ponts et Chaussées 190 (1994) 27–38.
[2] F. Lekarp, Permanent deformation behaviour of unbound granular materials, PhD thesis, Royal Institute of Technology, Stockholm, 1997.
[3] P. Hornych, A. Kazai, J.-M. Piau, Study of the resilient behaviour of unbound granular materials, in: V Conf. on Bearing Capacity of Roads and Airfields, Trondheim, 1998, pp. 1277–1287.
[4] COST 337, Unbound granular materials for road pavements, Final report of the Action, Transport research, European Commission, 2004.
[5] F. Mayoraz, Comportement mécanique des milieux granulaires sous sollicitations cycliques : application aux fondations de chaussées, PhD thesis n° 2488, Ecole Polytechnique Fédérale de Lausanne, 2001.
[6] F. Descoeudres, A.-G. Dumont, A. Parriaux, L. Vulliet, M. Dysli, P. Robyr, M. Fontana, G. Franciosi, Utilisation des matériaux d'excavation de tunnels dans le domaine routier, Etat des connaissances actuelles, ISRF-EPFL, mandat OFROU n° 52/98, 2000.
[7] VSS, SN_670-120 Graves pour couches de fondation, Exigences de qualité, Norme de la Vereinigung Schweizerischer Strassenfachleute, 1997.
[8] D. Luo, Image processing and pattern recognition, PhD thesis, University of Glasgow, 1995.
[9] R. Brewer, Fabric and Mineral Analysis of Soils, Wiley, New York, 1964.
[10] B. Cambou, Behaviour of Granular Materials, Springer, Berlin/New York, 1998.
[11] J. Biarez, P.Y. Hicher, Influence de la granulométrie et de son évolution par rupture de grains sur le comportement mécanique de matériaux granulaires, Revue française de génie civil 1 (4) (1997) 607–631.